J Mater Sci (2008) 43:5527–5533
DOI 10.1007/s10853-008-2839-z

The role of nanoquasicrystals on the ductility enhancement of as-extruded Mg–Zn–Gd alloy at elevated temperature

Yong Liu · Guangyin Yuan · Chen Lu · Wenjiang Ding · Jiangzhong Jiang

Received: 9 October 2007 / Accepted: 25 June 2008 / Published online: 9 July 2008

Abstract The microstructure and mechanical properties of Mg3.5Zn0.6Gd alloy containing quasicrystals was investigated after extrusion, the role of nanoquasicrystals on the ductility of alloy was analyzed. The results indicate that nanoquasicrystal was formed and distributed along grain boundary and in the matrix for Mg3.5Zn0.6Gd alloy after extrusion. As-extruded Mg3.5Zn0.6Gd alloy containing I-phase showed one relatively random and homogeneous texture due to the local lattice rotation during deformation. The Mg3.5Zn0.6Gd alloy extruded at 673 K exhibits larger elongation about 94% at 473 K, which could been ascribed to the combination of random texture and higher content of I-phase precipitated during extrusion at higher temperature. The $a + c$ type dislocations can be effectively active due to the existence of nanoquasicrystals. The strengthening mechanism of Mg3.5Zn0.6Gd alloy can be explained as the dislocations annihilation effect. This annihilation of dislocations can play a role in the increase of flow strain during deformation.

Y. Liu (✉) · J. Jiang
International Center for New-Structured Materials (ICNSM), Zhejiang University and Laboratory of New-Structured Materials, Department of Materials Science and Engineering, Zhejiang University, Hangzhou 310027, People's Republic of China
e-mail: liuyonggreg@yahoo.com.cn

G. Yuan · C. Lu · W. Ding
National Engineering Research Center of Light Alloy Net Forming, Shanghai Jiaotong University, 800 Dongchuan Road, Shanghai 200240, People's Republic of China

Introduction

Recently, Mg-based alloys reinforced with icosahedral quasicrystalline phase (I-phase) have been extensively studied, including many alloy systems, such as: Mg–Zn–Y [1–20], Mg–Zn–Gd [21–25], Mg–Zn–Ho [26], and Mg–Li–Zn–Y [27], etc. systems. The I-phase in these alloys was broken out and distributed along grain boundary and in the matrix as fine precipitates through thermo-mechanical processing, i.e. hot rolling [10–14], hot extrusion [3–9, 18–26], equal channel angular extrusion (ECAE) [15, 16], and severe hot rolling(SHR) [17]. Strengthening due to I-phase particles has been claimed since the I-phase particles are stable against coarsening and retain strength at high temperatures. These alloys show a good combination of strength and ductility, believed to be due to the strong interface between the I-phase and the Mg-matrix [11, 12], which comes from the very high symmetry and the unusual quasiperiodicity of the I-phase [6, 8, 26].

Especially, many researches [4, 11, 13, 16, 22] have focused on the deformability of alloys containing I-phase under elevated temperature, which has shown that the ductility of alloys could be improved greatly by the existence of I-phase particles, such as Mg4.3Zn0.7Y formed by ECAE [16] and Rolling [13] exhibiting super plasticity with about 600% and 556%, respectively.

In the present work, one Mg–Zn–Gd alloy containing nanoquasicrystal was studied through extrusion process. The role of nanoquasicrystals on ductility of Mg–Zn–Gd alloy was emphasized in the view of the interaction of I-phase and dislocation during deformation using TEM. The purpose of the present work is to understand the intrinsic cause for the large ductility of Mg–Zn–Gd alloy containing nanoquasicrystals.

Experimental

One alloy with the composition of Mg3.5Zn0.6Gd (at.%) was manufactured for this study. It was prepared by induction melting a mixture of high purity 99.9%Mg, 99.9%Zn, and 99.99%Gd in a mixed gas atmosphere of SF_6(1vol.%) and CO_2(99vol.%), and cast into a steel mold. The ingots were then machined into rods with a diameter of 100 mm and a length of 70 mm for extrusion. These rods were preheated inside the extrusion die for 1 h at the extrusion temperature before extrusion, and then extruded into a rod with a diameter of 30 mm, which corresponds to a reduction ratio of 11:1, and cooled in air. Extrusions were performed at two different temperatures of 573 K and 673 K. The tensile tests were performed at room temperature (RT) and 473 K on samples with a gauge length of 15 mm at strain rate 10^{-3} s^{-1}. Microstructure of alloys was investigated by X-ray diffraction (XRD) with the CuKα radiation, scanning electrical microscope (SEM) using Philips-Sirion200 attached with energy-dispersive spectroscopy (EDS), and transmission electron microscope (TEM) using a JEM-2010 operated at 200 kV. The sample for TEM was prepared by a standard combination of mechanical and ion-beam thinning technique.

Results and discussion

Microstructure of as-extruded alloy

The microstructure of as-cast Mg3.5Zn0.6Gd alloy has been shown in previous work [22]. This alloy formed a dendritic cast structure as hard skeleton in the matrix. The analysis of XRD exhibited that Mg3.5Zn0.6Gd alloy consisted of α-Mg and I-phase (quasilattice parameter $a = 0.520$ nm). The microstructures of Mg3.5Zn0.6Gd alloy extruded at 573 K and 673 K are shown in Fig. 1. As a result of extrusion, the I-phase in the interdendritic region of as-cast alloy was sharply destroyed and formed one black band structure along the extrusion direction. The mean grain size of the alloy extruded at 573 K was found to be about 4–8 μm, while the mean grain size of the alloy extruded at 673 K was found to be coarser, about 6–10 μm.

Figure 2 shows the TEM images of I-phase in Mg3.5Zn0.6Gd alloy extruded at 673 K. As shown in Fig. 2a, the dendritic phase formed in as-cast alloy was broken during deformation. Inset is its selected-area electron diffraction (SED) patterns showing fivefold axes, which indicates that the broken particle has the typical icosahedral quasicrystal structure. Figure 2b displays the TEM image of some particles with nanosize, which is precipitated along the grain boundary and in the matrix during extrusion process. The structure of nanoparticles was analyzed through the method of microdiffraction patterns, as shown in the inset of Fig. 2b. This microdiffraction patterns showed clearly a character of fivefold axes, therefore these nanoparticles could be confirmed as I-phase.

To further analyze the I-phase particle distribution in the matrix of as-extruded alloy, SEM observation with high magnification was carried out for alloy extruded at 573 K and 673 K, as shown in Fig. 3. It exhibits that the particle in the matrix of alloy extruded at 673 K is much fine and homogeneous as compared with those of alloy extruded at 573 K. The concentration of solute element in the matrix of alloy was tested through EDS analysis, as listed at Table 1. Alloy extruded at 573 K has solute concentration of about 4.78wt.% Zn and 1.48wt.% Gd in the matrix, while alloy extruded at 673 K has higher solute concentration of about 5.21wt.% Zn and 2.37wt.% Gd. The increment of Zn and Gd element is approximately 9% and 60%, respectively. It indicates that larger content of nanoquasicrystal precipitate can be obtained for alloy extruded at 673 K as compared with alloy extruded at 573 K. This may be attributed to the faster diffusion of solute atoms (Zn and Gd) and dynamical precipitate ability at high temperature, which affects the distribution and precipitation of particles in the matrix during extrusion process.

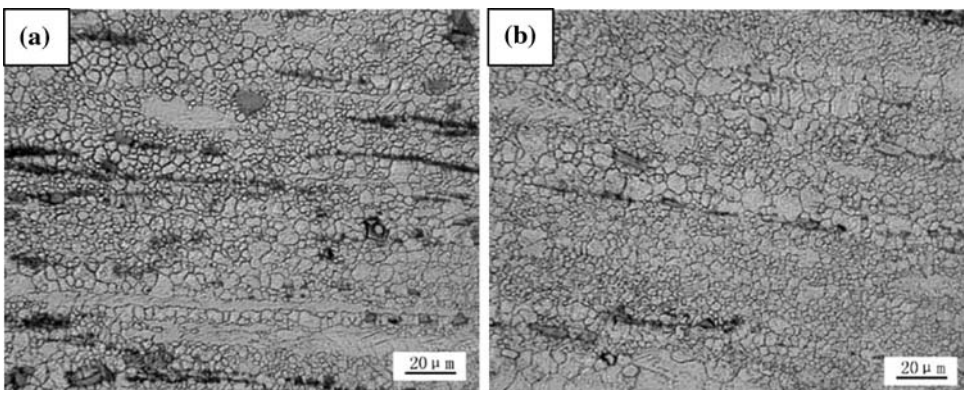

Fig. 1 Optical micrographs of the Mg3.5Zn0.6Gd alloy extruded at two temperatures (**a**) 573 K, (**b**) 673 K

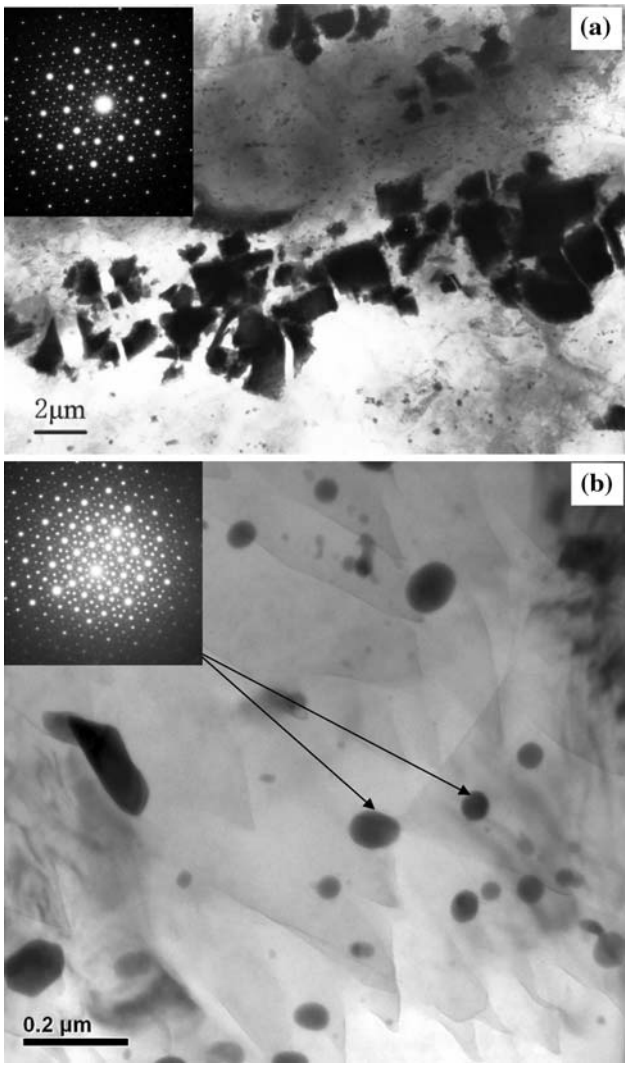

Fig. 2 TEM images of I-phase in Mg3.5Zn0.6Gd alloy extruded at 673 K. (**a**) Broken I-phase band with μm-scale size, inset is its SED patterns showing fivefold axes. (**b**) I-phase with nano-scale size along the grain boundary and in the matrix, inset is its microdiffraction patterns showing fivefold axes

Texture analysis

Texture plays an important role in the deformation of wrought Mg alloys. Figure 4 shows X-ray diffractions along and transverse to the extrusion direction of Mg3.5Zn0.6Gd alloy extruded at 673 K and 573 K. For alloy extruded at 673 K, the $(10\bar{1}0)$ peak of Mg is shown intense in the transverse direction and significantly weak in the parallel direction, while the (0001) peak of Mg is shown intense in the parallel direction. This is one common phenomenon called basal texture for Mg alloy with conventional extrusion process [28]. However, it is worth to point out that this basal texture is much weaker as compared with that of AZ31 after extrusion and more close to that of AZ31 prepared by ECAE process [28], which has a texture with 45°. In another words, one relatively random and homogeneous texture was formed for as-extruded Mg3.5Zn0.6Gd alloy containing I-phase particles, which was considered as a result of local lattice rotations and responsible for the good elongation in Mg–Zn–Y alloys strengthened by I-phase [29]. Here we have not found out the absence of the (0001) peak of Mg in the parallel direction, as reported by Singh et al. [8], which was considered as another factor responsible for the ductility of Mg–Zn–Y alloys containing I-phase.

As shown in Fig. 4, the XRD patterns of Mg3.5Zn0.6Gd alloy extruded at 573 K showed a similar texture distribution as compared with that of alloy extruded at 673 K.

Mechanical properties of alloy

Representative tensile stress–strain curves at room temperature (RT) and elevated temperature of as-extruded alloys are shown in Fig. 5. The mechanical properties at RT and 473 K of Mg3.5Zn0.6Gd alloy extruded at 573 K and 673 K are summarized in Table 2; for comparison, the properties of one Mg–Zn–Y alloy containing I-phase are also given from reference [4]. As shown in Fig. 5a, the

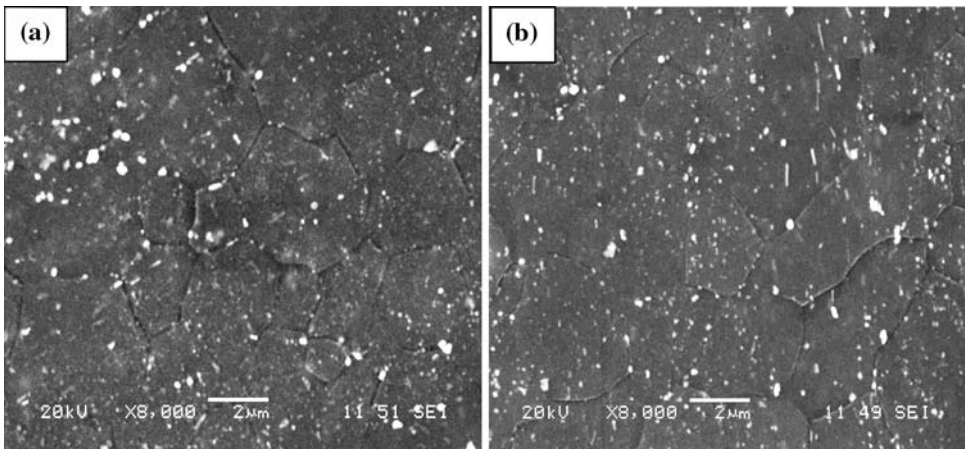

Fig. 3 SEM images with high magnification of Mg3.5Zn0.6Gd alloy extruded at two temperatures (**a**) 573 K, (**b**) 673 K

Table 1 Concentration of solute element in the matrix of Mg3.5Zn0.6Gd alloy after extrusion at 573 K and 673 K

Extrusion temperature	Composition in the matrix (wt %)		
	Zn	Gd	Mg
573 K	4.78	1.48	Bal.
673 K	5.21	2.37	Bal.

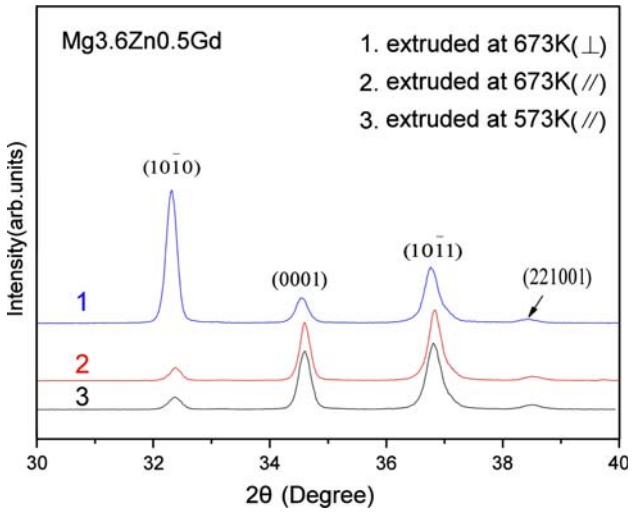

Fig. 4 X-ray diffraction from Mg3.5Zn0.6Gd alloy extruded at 673 K and 573 K on surfaces, perpendicular to and parallel to the extrusion direction

tensile mechanical properties at RT of the alloy extruded at 573 K are slightly higher than that of the alloy extruded at 673 K. The ultimate tensile strength (UTS), yield strength (YS), and total elongation of the alloy extruded at 573 K are about 311 MPa, 214 MPa, and 16.5%, respectively. These values of the alloy extruded at 673 K are decreased to about 302 MPa, 209 MPa, and 14.8%, respectively.

As shown in Fig. 5b, the Mg3.5Zn0.6Gd alloy extruded at 573 K and 673 K showed completely different stress–strain curve at 473 K. Although they exhibited similar UTS about 94 MPa and YS about 82 MPa, the Mg3.5Zn0.6Gd alloy extruded at 573 K and 673 K showed completely different total elongation at 473 K, the value of which is about 42% and 94%, respectively. This is one surprising phenomenon for the Mg3.5Zn0.6Gd alloy extruded at 573 K and 673 K, which has the same scale grain size, similar texture, and under completely the same test condition.

Interaction of nanoquasicrystal particles and dislocation

In order to analyze the interaction of I-phase and dislocation during deformation, the sample of alloy extruded at 673 K after tensile failure at 473 K was tested using TEM, as shown in Figs. 6 and 7. All TEM images in Figs. 6 and 7 are taken under two-beam diffraction conditions using different diffraction vectors, g, as indicated by arrows in the figures. The basal plane is aligned parallel to the incident beam direction, so that the basal plane can be seen edge-on. The basal-plane trace is indicated in each figure. Under this condition, straight dislocation segments lying parallel to the basal trace are in the basal-slip system, otherwise, dislocations are in the non-basal slip systems [30, 31].

Figure 6 shows the dislocation substructures taken with an incident electron beam direction of $[2\bar{1}\bar{1}0]$.As shown in Fig. 6, dislocations are visible in all three images taken under different two-beam conditions. As shown in Fig. 6b where $g = 0002$, the majority of dislocation segments are parallel to the basal-plane trace, suggesting that they are moving in the basal plane. However, the basal dislocation segments extend out of the basal-plane trace, as pointed with arrow in Fig. 6b, which indicates that there are some straight dislocations having c-component. These results exhibit that these dislocations belong to the $a + c$ dislocations, and can cross-slip from the basal plane to non-basal planes. As pointed with white arrows in Fig. 6c where $g = 01\bar{1}0$, some dislocations with a Burgers vector were observed around and bypass the I-phase particle. Figure 7 shows the dislocation substructures taken with an incident electron beam direction of $[10\bar{1}1]$. Dislocations are

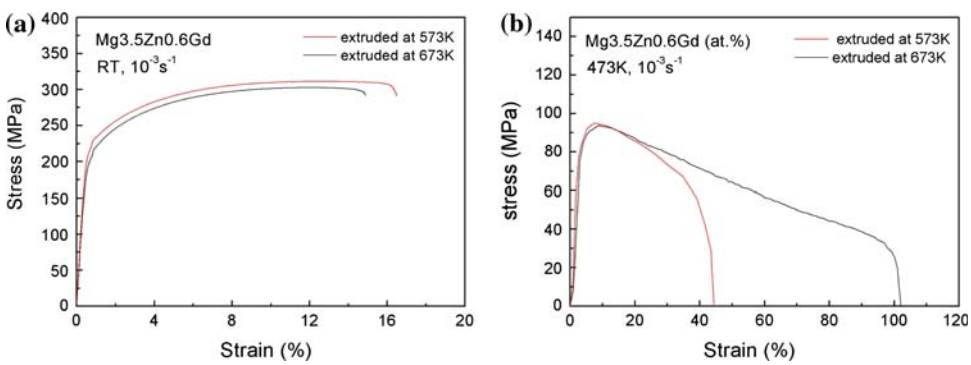

Fig. 5 Stress–strain curves of the Mg3.5Zn0.6Gd alloy extruded at 573 K and 673 K at two conditions. (**a**) RT, (**b**) 473 K

Table 2 Mechanical properties at RT and 473 K of Mg3.5Zn0.6Gd alloy after extrusion at 573 K and 673 K. (Strain rate: 10^{-3}/s)

Alloys (at.%)	Extrusion condition (K)	Mean grain size (μm)	RT			473 K		
			σ_b (MPa)	$\sigma_{0.2}$ (MPa)	ε (%)	σ_b (MPa)	$\sigma_{0.2}$ (MPa)	ε (%)
Mg3.5Zn0.6Gd	573	5	311	214	16.5	94	82	42
	673	8	302	199	14.6	91	79	94
Mg6.4ZnY [4]	523	10–15	315	210	20	170	140	41
	673	3–5	320	230	16	115	100	40

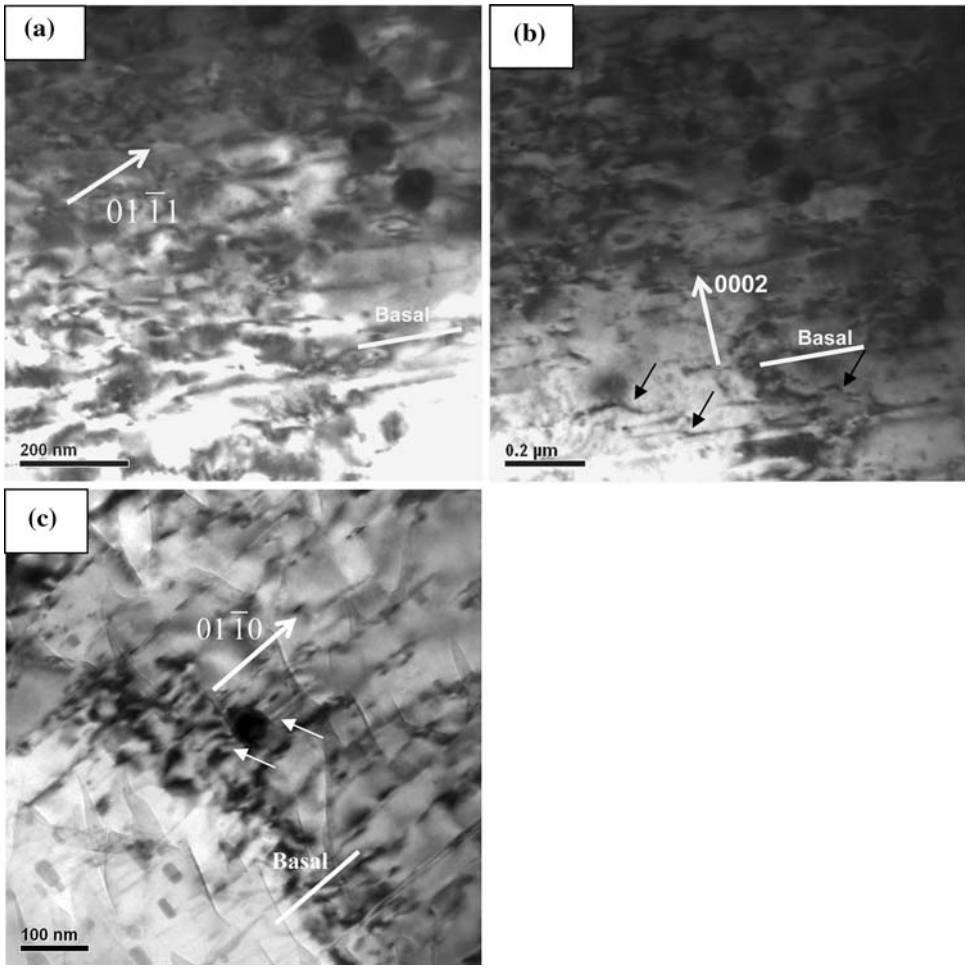

Fig. 6 The dislocation substructures of Mg3.5Zn0.6Gd alloy extruded at 673 K after tensile fracture at 473 K, which were taken with an incident electron beam direction of $[2\bar{1}\bar{1}0]$ under a two-beam diffraction condition with (**a**) $g = 01\bar{1}1$, (**b**) $g = 0002$, (**c**) $g = 01\bar{1}1$

invisible in Fig. 7a where $g = 0002$, which indicates all the dislocations have Burgers vectors of a type. The dislocations in Fig. 7b where $g = 1\bar{2}12$show that lot of $a + c$ dislocations were active and piled up around the I-phase particle, which denotes the operation of pyramidal slide system during the deformation.

Inoue et al. [32] has explained the strengthening mechanism of Al-based alloys containing nanoscale icosahedral particles using the Marting relation [33]. The origin of the Martin relation is similar to that for the Orowan relation [34]. Firstly, the dislocations are pilled up by the precipitation particles, but the subsequent dislocation can pass through by cutting the particles. When this concept is applied to the present alloy containing nanoquasicrystal particles, the dislocations are first piled up against the I-phase particles with nanosize, but the subsequent dislocations were annihilated at the interface between I-phase and matrix. This annihilation of dislocations at the interface seems to have similar action as that for the passage of dislocations by the precipitation particle, because the dislocations in these situations cannot play a role in the further increase in flow stress but flow strain. This mechanism gives a reasonable interpretation of high ductility of alloys with nanosize I-phase. Interfaces between the I-phase and matrix in Mg–Zn–Y alloys are reported to be quite strong [8]. The quasiperiodic property

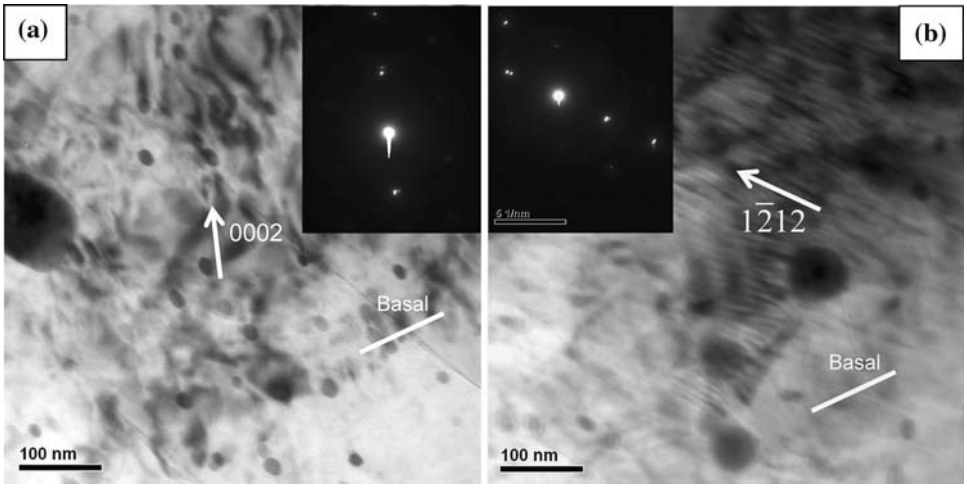

Fig. 7 The dislocation substructures of Mg3.5Zn0.6Gd alloy extruded at 673 K after tensile fracture at 473 K, which were taken with an incident electron beam direction of $[10\bar{1}1]$ under a two-beam diffraction condition with (**a**) $g = 0002$, (**b**) $g = 1\bar{2}12$. Inset is its corresponding two-beam diffraction patterns

of the I-phase ensures the formation of matching and strong interfaces with the matrix by creating several spacings on a set of planes. Singh and Tsai [35] pointed out that the I-phase has tendency to facet on fivefold and twofold planes. Therefore, the existence of nanoquasicrystals can effectively activate the $a + c$ dislocations responsible for the deformation of Mg alloy. This interesting phenomenon opened one inspiration that wrought Mg alloy with high ductility can be obtained through introducing large volume fraction of I-phase with nanosize in the matrix.

Conclusions

The microstructure and mechanical properties of Mg3.5Zn0.6Gd alloy extruded at 573 K and 673 K were studied. The role of nanoquasicrystals on the ductility of alloy was analyzed.

(1) The I-phase of as-cast Mg3.5Zn0.6Gd alloy was sharply destroyed through extrusion, and formed black band structure along the extrusion direction. There exist finer and larger content of I-phase particles in the matrix of alloy extruded at 673 K than alloy extruded at 573 K.

(2) As-extruded Mg3.5Zn0.6Gd alloy shows one relatively random and homogeneous texture, which was considered as a result of local lattice rotations and responsible for the good elongation of alloy strengthened by I-phase.

(3) The Mg3.5Zn0.6Gd alloy extruded at 673 K exhibits larger elongation about 94% at elevated temperature, which could be ascribed to the combination of random texture and higher content of I-phase precipitated during extrusion at higher temperature.

(4) The $a + c$ type dislocations can be effectively active due to the existence of nanoquasicrystals. The strengthening mechanism of alloy can be explained as the dislocations annihilation effect. The dislocations were first piled up against nanoquasicrystals, but the subsequent dislocations were annihilated at the interface between I-phase and matrix. This annihilation of dislocations cannot play a role in the further increase in flow stress but flow strain.

Acknowledgements This work was supported by National Natural Science Foundation of China (Num: 50501013) and Science and Technology Committee of Shanghai City (Num: 05JC14023). The authors are also thankful to the instrumental analysis center of shanghai Jiaotong University for the help of TEM observation.

References

1. Luo ZP, Zhang SQ, Tang YL (1993) Scr Metall Mater 28:1513. doi:10.1016/0956-716X(93)90584-F
2. Luo ZP, Zhang SQ (1993) J Mater Sci Lett 12:1490
3. Luo ZP, Song DY, Zhang SQ (1995) J Alloy Comp 230:109. doi:10.1016/0925-8388(95)01893-X
4. Singh A, Watanabe M, Kato A, Tsai AP (2004) Mater Sci Eng A 385:382
5. Singh A, Nakamura M, Watanabe M, Kato A, Tsai AP (2003) Scr Mater 49:417. doi:10.1016/S1359-6462(03)00305-1
6. Singh A, Tsai AP, Nakamura M, Watanabe M, Kato A (2003) Philos Mag Lett 83:543. doi:10.1080/09500830310001597027
7. Singh A, Watanabe M, Kato A, Tsai AP (2005) Acta Mater 53:4733. doi:10.1016/j.actamat.2005.06.026
8. Singh A, Watanabe M, Kato A, Tsai AP (2006) Philos Mag 86:951. doi:10.1080/14786430500253901
9. Singh A, Watanabe M, Kato A, Tsai AP (2005) Sci Technol Adv Mater 6:895. doi:10.1016/j.stam.2005.08.005
10. Bae DH, Kim SH, Kim WT, Kim DH (2001) Mater Trans MIT 42:2144. doi:10.2320/matertrans.42.2144
11. Bae DH, Kim SH, Kim WT, Kim DH (2002) Acta Mater 50:2343. doi:10.1016/S1359-6454(02)00067-8
12. Bae DH, Lee MH, Kim KT, Kim WT, Kim DH (2002) J Alloy Comp 342:445. doi:10.1016/S0925-8388(02)00273-6
13. Bae DH, Kim Y, Kim IJ (2006) Mater Lett 60:2190. doi:10.1016/j.matlet.2005.12.096

14. Lee JY, Lim HK, Kim DH, Kim WT, Kim DH (2007) Mater Sci Eng A 449–451:987
15. Zheng MY, Qiao XG, Xu SW, Wu K, Kamado S, Kojima Y (2005) J Mater Sci 40:2587
16. Zheng MY, Xu SW, Wu K, Kamado S, Kojima Y (2007) Mater Lett 61:4406. doi:10.1016/j.matlet.2007.02.013
17. Muller A, Garces G, Perez P, Adeva P (2007) J Alloy Comp 443:L1. doi:10.1016/j.jallcom.2006.10.006
18. Xu DK, Liu L, Xu YB, Han EH (2006) J Alloy Comp 426:155. doi:10.1016/j.jallcom.2006.02.035
19. Xu DK, Liu L, Xu YB, Han EH (2007) Mater Sci Eng A 443:248. doi:10.1016/j.msea.2006.08.037
20. Xu DK, Liu L, Xu YB, Han EH (2007) J Alloy Comp 432:129. doi:10.1016/j.jallcom.2006.05.123
21. Yuan GY, Kato H, Amiya K, Inoue A (2005) J Mater Res 20:1278. doi:10.1557/JMR.2005.0156
22. Liu Y, Yuan GY, Lu C, Ding WJ (2007) J Alloy Comp 427:160. doi:10.1016/j.jallcom.2006.03.027
23. Liu Y, Yuan GY, Lu C, Ding WJ (2006) Scr Mater 55:919. doi:10.1016/j.scriptamat.2006.07.035
24. Liu Y, Yuan GY, Lu C, Ding WJ (2007) Mater Sci Forum 546–549:323
25. Yuan GY, Liu Y, Lu C, Ding W (2008) Mater Sci Eng A 472:75. doi:10.1016/j.msea.2007.03.016
26. Singh A, Somekawa H, Mukai T (2007) Scr Mater 56:935. doi:10.1016/j.scriptamat.2007.02.015
27. Xu DK, Liu L, Xu YB, Han EH (2007) Scr Mater 57:285. doi:10.1016/j.scriptamat.2007.03.017
28. Mukai T, Yamonoi M, Watanabe H, Higashi K (2001) Scr Mater 45:89. doi:10.1016/S1359-6462(01)00996-4
29. Lee JY et al (2008) Mater Sci Eng A. doi:10.1016/j.msea.2008.02.010
30. Suzuki M, Sato H, Maruyama K, Oikawa H (2001) Mater Sci Eng A 319–321:751. doi:10.1016/S0921-5093(01)01005-X
31. Koike J, Kobayashi T, Mukai T, Watanabe H, Suzuki M, Maruyama K et al (2003) Acta Mater 51:2055. doi:10.1016/S1359-6454(03)00005-3
32. Inoue A, Kimura H (2000) Mater Sci Eng A 286:1. doi:10.1016/S0921-5093(00)00656-0
33. Martin JW (1980) In: Micromechanisms in particle-hardened alloys, Cambridge University Press, Cambridge, p 62
34. Orowan E (1934) Z Phys 89:614. doi:10.1007/BF01341479
35. Singh A, Tsai AP (2005) Scr Mater 53:1083. doi:10.1016/j.scriptamat.2005.06.041